Aus dem Department für Augenheilkunde Tübingen
Universitäts-Augenklinik
Schwerpunkt: Neuro-Ophthalmologie
Ärztlicher Direktor: Professor Dr. E. Zrenner

Alterskorrelierte Normwerte der Lichtunterschiedsempfindlichkeit für die automatische statische Rasterperimetrie mit dem Octopus 101-Gerät

Inaugural-Dissertation
zur Erlangung des Doktorgrades
der Medizin

der Medizinischen Fakultät
der Eberhard-Karls-Universität
zu Tübingen

vorgelegt von
Agness Matthiesen, geb. Hermann

aus

Pawlodar/Kasachstan

2008

Dekan:	Professor Dr. I. B. Autenrieth
1. Berichterstatter:	Professor Dr. U. Schiefer
2. Berichterstatter:	Professor Dr. K. Dietz

Meinen Eltern
und meinem lieben Mann Benedikt

Inhaltsverzeichnis:

Age-dependent normative values of differential luminance sensitivity in automated static perimetry of the Octopus 101-instrument

Agnes Matthiesen[1], Jens Paetzold, Dr. rer. nat. (co-author, consultant)[1a], Reinhard Vonthein, Dr. rer. pol. (statistician)[2], Elke Krapp[1], Bettina Selig[1], Stephan Rauscher[1], Ulrich Schiefer, Prof. Dr. med. (senior co-author)[1a*].

[1] Centre for Ophthalmology, University of Tuebingen, Germany

[2] Department of Medical Biometry, University of Tuebingen, Germany

[a] Financial disclosure: consultant of Haag-Streit, Koeniz, Switzerland

* Corresponding author:
Prof. Dr. med. Ulrich Schiefer
Centre for Ophthalmology, University of Tuebingen
Schleichstr. 12-16, D-72076 Tuebingen, Germany
Phone: ++49 – 7071 29-87429
FAX: ++49 – 7071 29-5038
Email: ulrich.schiefer@med.uni-tuebingen.de

Abstract

Purpose: To determine age-dependent normative differential threshold values for the Octopus 101-instrument and to create a smooth mathematical model characterizing the age-dependency and the asymmetry of the hill of vision.

Methods: Static automated perimetry within the central 30° visual field was conducted with the Octopus 101-instrument in 81 eyes of 81 ophthalmologically healthy subjects (11 – 12 per decade of age) from 10 to 79 years. To obtain threshold values a 4-2-2 stair-casing strategy with 3 reversals was run. The test point grid consisted of 68 concentrically arranged points with test point condensation towards the visual field centre, representing the approximately rotation symmetric 30°-hill of vision. Background luminance was kept constant at 10 cd/m^2. Thresholds of differential luminance sensitivity (DLS) were estimated by the maximum-likelihood method. A smooth mathematical model was fitted to the normative data.

Results: The model fit was satisfactory (R^2= 0.74). Co-variables defining the model were: age, eccentricity, angle and subject. Total random standard deviation was 1.75 dB. The residual standard deviation exceeded 1.75 dB in the border region of the 30° visual field, was 1.5 dB within the centre and fell below 1.25 dB in a ring around the centre. Average thresholds of the visual field varied with age like: $DLS = \frac{0.495\,\mathrm{dB}}{\mathrm{decade}} \times age - \frac{0.112\ \mathrm{dB}}{\mathrm{decade}^2} \times age^2$, which is close to constant from 10 to 40 years and declines ever steeper thereafter. The effect of age on the DLS in the visual field increased with eccentricity. The greatest drop was in the peripheral superior hemifield: At an eccentricity of 25° the superior DLS was estimated to be 5.5 dB higher in 10 year olds than in 75 year olds.

Conclusions: This new smooth model allows to predict age-related normal threshold values for any stimulus location within the 30° visual field and thus to compute global and local measures of defect like mean defect or p-values for any kind of stimulus arrangements.

Key words*:* automated static perimetry, visual field, normative values, mathematical model.

Introduction

The exact knowledge of age-related normative values of differential luminance sensitivity (DLS) is an essential prerequisite for any kind of threshold-related visual field testing. In order to maximize the diagnostic information benefit, optimal test conditions are desired: optimized test point density, spatial distribution and number of test point locations. Approaches like fine grid perimetry or the interlocking grids like the 30-1 and 30-2 test of Humphrey perimeters or the 31 and the 32 programs of the Octopus instrument indeed show a high spatial resolution, but do have the considerable disadvantage of an expenditure of time [23,66,67]. The rectangular test point arrangements of the classic grids, which are predominantly used so far, only inadequately consider the pattern of the retinal receptor and ganglion cell distribution [62,77]. Furthermore, the visual field centre, representing the foveola with the maximum DLS and thus very important diagnostic details are ignored in this type of grid. For the detection and follow-up of glaucomatous visual field damages a detailed test point arrangement in suspected scotoma regions is desirable. Based on the determination of the most frequently affected areas in glaucomatous visual field loss, some demands for the most suitable test point arrangement were established: test point condensation towards the centre with involvement of macula [23,77] test location distribution in the periphery between 20° and 30° of eccentricity [68,80] and sufficient test locations in the nasal, superior paracentral (Bjerrum) and blind spot area [25,55,80].

Perimetric grids with individually condensed stimulus locations in “regions of interest” (i.e. at the scotomas borders) are a promising option for an efficient delineation and follow-up of glaucomatous visual field loss [59]. An optimized grid was initially developed [59-62] on a prototype campimeter (Tübingen Computer Campimeter [74]). This test point arrangement was an approach to reflect the physiological visual field characteristics (like distribution of photoreceptors) as well as to take into account the above-mentioned knowledge of glaucomatous visual fields. Due to previous results the included test location number of 68 points should be sufficient enough to reach a high precision

(sensitivity and specificity) [28]. The great capabilities of TCC, being able to offer any stimulus arrangement within the central 30° of the visual field and to adapt test point grids to the individual pathology, have been transferred recently to the commercially available Octopus 101-perimeter (Haag-Streit Inc., Koeniz, Switzerland) [33], requiring a new normative age-dependent data set [41].

The purpose of this study was to determine age-specific normative values of differential luminance sensitivity (DLS) for the Octopus 101-perimeter and to describe these by a smooth mathematical model, considering the age-dependency and quantifying the asymmetry of the hill of vision.

Subjects and Methods

Participants

We examined 81 eyes of 81 ophthalmologically healthy subjects (41 females, 40 males, ages from 10 to 79 years) with 11-12 individuals per decade. The participants were recruited from the general public from the Tuebingen region of Germany. They were members of church parishes, senior citizens from retirement homes, passers-by in Tuebingen`s pedestrian zone and friends or relatives of the employees. They were selected to represent as broad a cross section as possible of all social levels. Written informed consent of each volunteer was obtained. Each subject underwent an ophthalmic examination and had to meet the following inclusion criteria: maximum distance spherical ametropia ± 6.00 Dsph, maximum cylindrical ametropia ± 2.00 Dcyl, best corrected distance and near visual acuities (Birkhaeuser reading test, Birkhaeuser Verlag, Basel) ≥ 1.0 (20/20) for the age group < 60 years, ≥ 0.8 (16/20) for those aged between 61 to 70 years, and ≥ 0.63 (12/20) for the age group > 70 years. All subjects manifested normal LANG(I) stereo test (Lang, Forch, Switzerland), equal pupil diameter (isocoria), normal ocular motility (no double vision), normal anterior segments (no relevant opacities of central refractive media), normal fundus (examination with undilated pupils, after perimetry), intraocular pressure (IOP) ≤ 22 mm Hg (air pulse tonometry, performed after perimetry), no intraocular trauma or inflammation, no eye surgery (except intraocular lens implantation without any known complication), no squint, amblyopia, patching, penalization, nystagmus, no hint of visual pathway lesions, no manifest strabismus, no relative afferent pupillary defect. Exclusion criteria were diabetes mellitus, current arterial hypertension (RR > 180/90 mmHg) or other systemic diseases, hint of intracerebral pathology, drugs potentially affecting reaction time, alcohol, nicotine or caffeine less than 2 hours before perimetric examination. Leading and non-leading eyes were determined with Rosenbach`s fixation test [57], 39 right and 42 left eyes were entered into the study. All subjects had a rested, relaxed condition.

Approximately 60 % of the participants concluded 1-2 prior perimetric normative value testings, before being examined in this study. The other subjects never had any perimetric examinations before. All procedures, including the protection of the subjects` privacy were in compliance with the Declaration of Helsinki and were approved by the local Independent Ethics Committee.
Persons exceeding an incorrect response rate of 20 % of the false-positive or false negative catch trials were excluded from the study.

Technical data and examination procedure

The Octopus 101-perimeter [33] uses a conventional projection system, the cupula radius is 45 cm, background luminance was set to 10 cd/m². White stimuli with the standard size of Goldmann III (26`) were used and presented in randomised order, stimulus duration was fixed at 100 ms. The interval between the stimuli presentations (inter–stimulus interval) was set to 1500 ms. Before starting the examination, a short training program containing 10 different target locations was presented. To minimize the influence of participants´ fatigue, the examination was interrupted every 4 minutes for 2 minutes. The test point grid (68 stimulus locations) within the central 30° is shown in Fig.1: Stimuli were arranged in a circular, approximately rotation symmetrical order with a test point condensation towards the centre. A 4-2-2 dB staircase strategy with 3 reversals was run. Regarding quality control, 5% of all stimuli were presented as false-positive, and 5% as false-negative catch trials [73]. An integrated infrared camera was used for fixation control, recording the patient's eye's movements and blinking. The Octopus 101-perimeter interrupted automatically, if the pupil moved outside the predetermined position. When blinking occurred during a stimulus presentation, the stimulus was repeated automatically. The examiner observed the position of the subject's eye and fixation behavior and alerted the subjects in case of suspected reduced vigilance.

Analyses

The stimulus within the blind spot was excluded from the evaluation. The coordinates of the left eyes were mirrored at the vertical meridian. The two

points above and below the blind spot were inside the blind spot in some patients. They were excluded, if their DLS was 2 dB less than the DLS of the contiguous peripheral points.

A smooth mathematical model was estimated [46,63] to describe the normative threshold values, which allows to predict DLS at any location of the "hill of vision". Modeling the hill of vision was performed, based on the following assumptions (see Schwabe [63]):

"1. The pupil, retina and fovea are round (oval) with a common center. 2. Radial cross-sections reveal that the steepest ascent of differential luminance sensitivity occurs near the edge of the 30° visual field. 3. On central cross-sections, the fovea is represented by a sharp peak of different luminance sensitivity. 4. The isopters of DLS are more extended in the temporal than in the nasal hemisphere, in the inferior than in the superior hemisphere, in the nasal than in the inferior hemisphere. 5. Elderly persons show a somewhat reduced visual performance. 6. The aging process affects the center and periphery differently. 7. Elderly persons suffer relative visual constriction, which results in a steeper descent of DLS towards the periphery."

Four variables (age, eccentricity, angle and subject) were entered into the model. The interaction terms were checked for reasonable magnitude of effect via the analysis of variance table (JMP software, version 5.1, SAS Institute Inc., Cary NC 2003). This was realized by regarding the sums of squares and the significance (inclusion if $p < 0.05$) of an interaction term and the adjusted R^2 (coefficient of determination, indicating the percentage of the variance of the measured values that can be explained by the model). Only those interaction terms were included in the model, which increased the adjusted R^2. If one interaction term containing the sine of the angle increased R^2, the corresponding term with the cosine was included, too, and vice versa [46,63]. If an interaction of higher order improved the quality of the model, interactions of lower orders were incorporated also.

The most salient features of the model were captured with fewer parameters to develop a further parsimonious model. Occam´s razor was applied by elimination of all terms with sums of squares smaller than 15.

Results

Participants / Analyses

Nine of the initially enrolled subjects had to be excluded afterwards due to > 20 % of false positive catch trials. One of the contiguous blind spot points was excluded in 43 subjects as described above.

Estimation of the model

This model is based on two mathematical methods: Interpolation between the test points and approximation of expected values. A detailed description is given in the Appendix.

Model fit can be ruled as satisfactory ($R^2 = 0.74$), indicating that the variance of predicted values accounts for 74 % of the variance of the measured values. As the adjusted R^2 is equal to R^2, it can be assumed that no meaningless factors were included. RMSE (= Root Mean Square Error), estimating the standard deviation (SD), i.e. the intra-individual variation, was 1.426 dB. As local threshold was evaluated in 1 dB steps, this standard deviation (SD) is acceptable being in the same order of magnitude. The variance components were analysed as:

Variance = (Standard Deviation $_{total})^2 = (SD_{total})^2 = (SD_{intra})^2 + (SD_{inter})^2$ or
$(1.75\ dB)^2 = (1.43\ dB)^2 + (1.01\ dB)^2$.
Total random variance $(SD_{total})^2$ is $(1.75\ dB)^2$. $(SD_{intra})^2$ is the variance of the residual, which is attributable to measurement error and is $(1.43\ dB)^2$. $(SD_{inter})^2$ is the variance attributable to the individual (subject) and is $(1.01\ dB)^2$. (The fractions of the total standard deviation were approximated to the second decimal place). The variance of the measurement is approximately twice the intra-individual variance.
The simpler model had R^2 and adjusted $R^2 = 0.736$ each, residual SD = 1.44, detailed description is given in the Appendix too.

Varying precision in the visual field and across ages

Figure 2 presents the residual standard deviation across the visual field. The residual standard deviation is highest in the border region of the 30° visual field (residual SD ≥ 1.75 dB), intermediate in the centre (residual SD ≈ 1.5 dB) and smallest in a ring around the centre (residual SD ≤ 1.25 dB). In the nasal part of the visual field there is a smaller residual standard deviation than in the temporal one. In the superior rim region of the visual field, where the position of the upper eye lid is becoming relevant, the residual standard deviation comes close to 2 dB. The dependence of the residual threshold standard deviation on age can be described by the quadratic function:

$$SD_{\text{residual threshold}}(age) = 1.27665\ \text{dB} - \frac{0.00314\,\text{dB}}{\text{year}} \times age + \frac{0.00011\,\text{dB}}{\text{year}^2} \times age^2.$$

The residual standard deviation of 10 years olds is 1.26 dB and of 79 years olds is 1.72 dB.

Ageing

From the analysis of the recorded threshold data it can be derived that the DLS decreases with age in a non-linear way (Fig.3). Average DLS varies with age like $DLS = \frac{0.495\,\text{dB}}{\text{decade}} \times age - \frac{0.112\ \text{dB}}{\text{decade}^2} \times age^2$, which is close to constant from 10 to 40 years and declines ever steeper thereafter. In order to estimate the DLS decrease with age, we computed the derivative of the quadratic function of age in the centre. Threshold values of the third decade of life are higher than those of first and second decade, especially towards the periphery. Analyzing the aging process as a function of location, we find a larger and more rapid pace of ageing peripherally (Fig.3/4).

Asymmetry

Considering the *vertical* profile section (90°-270°) of the hill of vision (Fig.5), in the entire 30° visual field the inferior DLS is higher than in the superior one. Asymmetry is increasing towards the periphery (10°: 0.5 dB; 20°: 1.0 dB; 25°:

1.3 dB). In the *horizontal* profile section (0°-180°) of the hill of vision (Fig.5) up to an eccentricity of about 20° the DLS is slightly higher in the nasal hemisphere than in the temporal one. When exceeding an eccentricity of approximately 20°, the situation is reversed. The greatest naso-temporal asymmetry (2 dB) occurs at an eccentricity of 30°. The age effect on the DLS asymmetry in the visual field increases with eccentricity (Fig.6). The greatest DLS decrease occurs at the border of the superior hemifield (25°). DLS is estimated to be 5.5 dB higher in 10 year olds than in 75 year olds. At the horizontal meridian our results show only slight difference in the effect of aging on DLS between the nasal and the temporal hemispheres (Fig.6).

Discussion

In the vast majority of previous normative studies, two different approaches were undertaken in order to assess normative threshold values: a) an attempt to appraise the hill of vision at each test location of the stimulus grid individually [4,24,34,40,63,81], disregarding the correlation between neighbouring points [41,63] or b) visual field indices were introduced for averaging of threshold values over certain visual field areas [27,37,42,63,82], but missing local characteristics of the visual field. In this study a mathematical model was used [46,63] for describing all tested points of all examined subjects. This was done to overcome the above-mentioned deficits by interpolating between test point locations [41,63]. Thus normative values for locations, which are not included in the grid [62] can be mathematically derived and local asymmetries can be taken into account.

Model

Comparing our results with similar modeling approaches of Schwabe [63] and Lorch [46], we could achieve the greatest model fit. The main reason for the high adjusted R^2 can be attributed to the additional introduction of the factor “subject”. In this way a random effect of subjects is taken into account. When setting this factor aside, we obtain an adjusted R^2, which is somewhat lower than in Schwabe´s - and higher than in Lorch´s study. A possible explanation for the rather greater uncertainty in Lorch`s model is the high variability of the data, attributed to the use of the 4-2 strategy [46]. DLS, which is obtained with a more detailed staircase strategy (4-2-2 in our study or 4-2-1 in Schwabe´s study [63]) and calculated on the basis of the maximum-likelihood method, shows a smaller variability, resulting in an increasing R^2. In contrast to Schwabe`s model, we include a further interaction between eccentricity, the cosine and sine of two times the angle and age, which describe an ellipse, flatting the isopters horizontally, depending on age. Further attempts to model the hill of vision could not be found in the literature.

Parsimonious model

The model could be reduced to ten systematic effects (including individual coefficient). All physiological characteristics of the hill of vision are still realized in this model. Due to the simplicity of the model there is some loss of quality. R^2 declined by 0.004 and residual SD increased by 1%.

We applied the more complex model, as it was constructed to respect commonly accepted statistical practice: significance, adjusted R^2, inclusion of main effects, when interactions are included, for agreement with specifications set up in previous research. It presents a higher precision (although slight) and a higher flexibility to detect deviations, when applied to other populations. For practical purposes the parsimonious model will suffice and prove more robust in small samples.

Varying precision in the visual field and across ages

As shown in Fig.2 we found an increasing residual standard deviation towards the periphery and a decreasing residual standard deviation towards the centre. An increasing inter- and intra-individual variability with increasing eccentricity has been described before [26,30,37,44,53,78]. The increment of variability with eccentricity within one subject and thus the increase of the residual standard deviation may be ascribed to anatomical circumstances (see below) and to the physiological decrement of photoreceptors towards the periphery and the depression in neuroretinal sensitivity there. The variability between individuals can be explained by the different slopes in their hills of vision. Within the central 5° we found a higher residual standard deviation than in the pericentral area. Due to the steep slope of the hill of vision in this area, even minor deviations of fixation result in a significant increase of variability, and consequently a higher residual standard deviation. The greatest residual standard deviation is localized in the superior hemifield. This is in a good agreement with previously published results, showing greatest variability in the superior visual field [37,38]. This fact is explained by the variability of upper eye lid position [37]. The inter-individual variability might be due to the different eye lid and orbit rim

configuration among subjects, whereas the intra-individual variability might be explained by the different eye lid positions of one subject during the test. In the intermediate nasal part of visual field we observe less residual standard deviation and therefore less variability as in the temporal half. The reason for this conclusion may be the small number of measurements in the temporal field, as the blind spot area was excluded. The increase of variability in the lower nasal sector of the 30° visual field is most probably related to anatomical variability. We find that age increases the residual standard deviation. This confirms the result of the increasing variability with age in previous literature [38,49]. Except the blind spot, the model fit is of the same quality in all locations of the visual field. The minimum and maximum residual threshold standard deviation in the visual field differs by less than 38%. The width between the reference limits should vary accordingly. This is of clinical relevance, as a constant width results in too many flagged points peripherally and too few at intermediate eccentricities.

Ageing

Up to now the aging process is not completely understood. There are several factors which can account for the age-related visual field sensitivity loss. Findings of previous studies disagree in this concern. Some of the investigators attributed the normal age-related sensitivity decline to the age-related changes in the preretinal structures [19,27,42]. Changes in the transmission properties of the ocular media [7,10,50,54,58,64,71,79] as well as age-related reductions in pupil size might be responsible for threshold depression with age [16,76]. However some of the researchers emphasized the importance of the age-related neural losses. Johnson [36], who minimized the influence of lenticular transmission losses and pupil size in his study by screening the subjects carefully in regard to refractive opacities, found that normal age-related visual field sensitivity change are primarily due to neural cell losses rather than to preretinal factors. Weale [75], who originally ascribed the major portion of the age-related visual field DLS losses to preretinal factors suggested later that the cell loss within the central optic pathway is the major factor in the explanation of

the sensitivity decline with age [76]. Many histological studies have shown that age-related reductions in photoreceptors density [9,15,21,22,48], photopigment density [39,70], the number and morphology of the optic nerve axons [2,14,56,65] and population density of neurons in the visual cortex [12] do exist. Both, preretinal and neural age-related degenerations have an effect on the age-related visual field sensitivity loss. However it is still impossible to determine the relative contribution of these factors in the aging visual system. Further controversy exists in the understanding of the DLS decline with age: Diverse studies assumed a linear decrease of threshold values with age [4,16,17,19,20,27,29,30,35,40,51,81], whereas many authors found a change point, demonstrating an increasing loss of sensitivity at a specific age [11,34,42,43,46,63,72]. To explain the discrepancy of a continuous loss of sensitivity and an accelerated loss at older ages, Lachenmayr [42] scrutinized the inclusion criteria for visual acuity in previous normative studies. He noticed, that studies reporting an accelerated loss at an older age [34,42] used a stricter acuity criterion. However Okuyama [51], who included only subjects with a vision of 20/20, claimed a linear loss of sensitivity. It is conspicuous, that studies, which found a linear sensitivity decrease, show some shortcomings in the study design. For instance, Jaffe [35] reported on a total sample size of only 25 participants. Haas [27] enrolled 153 volunteers (203 eyes), with a disproportionate number of young subjects. Brenton [4] chose subjects who were older than 20 years, recruiting also department employees. Another plausible explanation might be found in the applied analytical methods by Iwase [34]. He pointed out that evaluations, based on a linear regression, ignore the non-linear decay of DLS, supporting the theory that the visual field remains stable up to a certain age and then deteriorates.

This concept is in good agreement with corresponding previous reports on normal age-related preretinal and neural changes. Said [58] and Tan [69] showed that hardly any changes in the transmission properties of the ocular media occur between 5 and 30 years of age. After 30 years of age a process of yellowing of the crystalline lens starts. From the Duane`s [18] accommodation amplitude curve it can be concluded that the accommodation capability

deteriorates up to the age of 50 and 60 years. Thenceforth the accommodation capability keeps approximately stable. Marshall [48] demonstrated a change with aging in human photoreceptors, starting at the age of 40 years. Gartner [22] found an displacement of the nuclei of photoreceptors from the outer nuclear layer both into the outer plexiform layer (increasing after age 30, and most pronounced after age 50), and into the layer of rods and cones (after age 40 years, most common after age 50 years). Van Norren [70], who investigated the density of human cone pigments as a function of age, could not find any significant change in density up to 50 years. However he assumed a cone pigment density loss beyond 50 years. Gao [21] assessed an age-related rod and ganglion cell layer loss, being most pronounced between the second and the forth decade. Dolman [14] reported on a loss of axons with increasing age, particularly marked from 60 years. Devaney [12] ascertained that the population density of neurons in the visual cortex falls mainly between the third and the sixth decade.

Our results support a non-linear aging process. The DLS was nearly constant irrespective of age until the age of 30 to 40 years and then declined in an accelerated manner with age. A slight increase during adolescence could be explained by better cooperation. We must emphasize that these results are derived from a cross-sectional study. To be able to understand the aging process better and to avoid bias effects longitudinal studies are needed certainly, which could demonstrate the physiological decrease of the DLS over years [6].

Asymmetry

Superior-inferior asymmetry

In previous investigations [3,4,5,13,16,30,37,46,81] sensitivity is reported to be lower in the superior hemifield than in the inferior one. Our results confirm this for all decades, showing that the inferior-superior asymmetry increases almost linearly towards the periphery (Fig.5). We are in agreement with Katz [37], who observed that the slope of the hill of vision with increasing eccentricity is greatest in the superior area. Some investigators reported on a higher DLS

decrease with age in the upper hemifield [5,13,27,37,63]. Dietrich [1,13] and Ata [1,13], using a linear regression for the evaluation, found a higher sensitivity of about 0.3 dB in the lower half of the visual field already in ten-years old, the difference increasing by 0.14 dB per decade.

Our data agree with these findings: DLS depression with age is more pronounced in the superior visual field than in the inferior one. Especially in the periphery (25°) a greater aging effect was observed (Fig.6). Up to now the reason for the asymmetric depression in the superior half of the visual field is not completely understood. Physiological phenomena may be one reason for this observation. Curcio [8], who investigated the topography of ganglion cells in the human retina, found a higher ganglion cell density in the superior part of the retina than in the inferior one. Another explanation could also be the greater luminance of the sky above the horizon, causing greater adaption in the upper visual field, corresponding to the lower hemiretina. Moreover eye lid artifacts in this area are known and cause a shadowing of the superior visual field [13,37], especially with increasing age. Katz [37,38] attributed the lower DLS in the superior hemifield to blinking.

Naso-temporal asymmetry

Concerning the naso-temporal asymmetry in the visual field our findings are consistent with the results of Lorch [46] and Schwabe [63]: Up to the eccentricity of 20° the nasal DLS is higher than the temporal one. From 20° the situation reverses (Fig.5). These findings are concordant with Curcio`s [8], showing in the peripheral nasal part of the retina a higher ganglion cell density than in the temporal retina. In the past, some investigators could observe a greater influence of age on the temporal hemifield [13,19,45,46]. Dietrich [13] showed a reversal of the naso-temporal asymmetry at the age of 40 years benefiting the nasal hemifield. Lewis [45] reported on a higher sensitivity of the temporal part of the visual field in children. As explanation Dietrich [13] discussed the anatomical conditions in the periorbital region: The greater exposure of the nasal retina to light causes an earlier retinal maturation and may also result in a greater aging effect in this area. However the method, which Dietrich [13] used in his analysis is problematic. Lorch [46] advised

against Dietrich`s “mean value method”, averaging over the entire visual field. Using the mathematical model we could not find any greater differences in the effect of aging between the nasal and temporal hemifield. The greatest difference between the DLS decrease with age in the nasal and the temporal hemifield was 0.64 dB, benefiting the temporal quadrant. This is below the measuring accuracy of 1 dB and therefore negligible. In this point we conform to Katz [37], who also could not detect any statistically significant hemifield-related differences in the influence of age.

Generalisability

In our randomized, balanced and stratified study we enrolled a fairly large, representative sample of ophthalmologically healthy subjects. About two thirds of our participants concluded maximum two perimetric testings before being examined in our study. The remaining subjects did not have any contact to perimetry before. In previous literature it was found, that the majority of subjects shows reliable results already in their first perimetric session [31,47]. However, there is also an important minority among normal and pathological eyes, presenting a dramatic DLS increment with perimetric training, especially in the first tests [52]. Heijl [31] admonishes of a very wide normative values range, if reference limits were estimated from inexperienced volunteers, producing low DLS peripherally and concentric constriction. He postulates, that initial fields, being contradictory with clinical findings, should be retested. A potential bias of conceivable learning effects in our study was taken into account by a proportionate distribution of perimetrically “experienced” individuals. In order to minimize the existing difference between the non-learners and learners, the participants were subjected to a short training program. Largely the perimetric experience of our subjects is representative of a population in a normal clinical setting. The interaction of the learning and fatigue effect is still not completely understood [32]. In order to reduce the influence of the fatigue effect, which may decrease sensitivity during an examination [32], after 4 minutes testing time, rest periods of 2 minutes were inserted. Furthermore the total examination duration (including breaks) was on average 21 minutes and not longer than 26

minutes. Concerning the external validity of the applied model, of course serial measurements and larger sample of subjects are needed to prove it. However, considering studies with similar study design and application of similar models [46,63], we must point out, that the reported results on model fit, DLS asymmetries in the visual field and the aging process are comparable with our findings. Consequently we assume, that our model as well as our trial findings are generalisable and applicable for clinical purposes.

Conclusion

The development of a smooth mathematical model based on an optimized examination grid allows for prediction of age-corrected normal DLS values at any given stimulus location within the central 30° visual field.

Figures and Legends

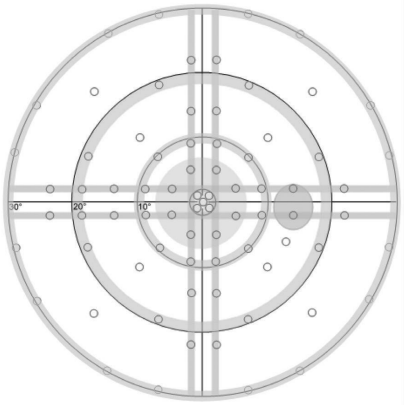

Fig.1: Optimized 30°- test location pattern (right eye). Test points are located approximately rotation symmetrically, in a circular order with para-axial locations (2.5°distance from the main axis) and a stimulus condensation towards the center.

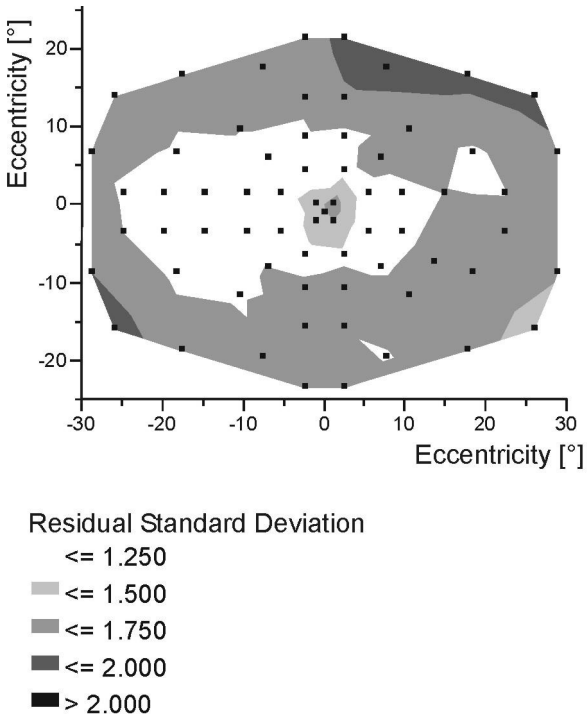

Fig.2: Residual standard deviation (right eye): It is highest in the periphery, average in the centre and smallest in a ring around the centre.

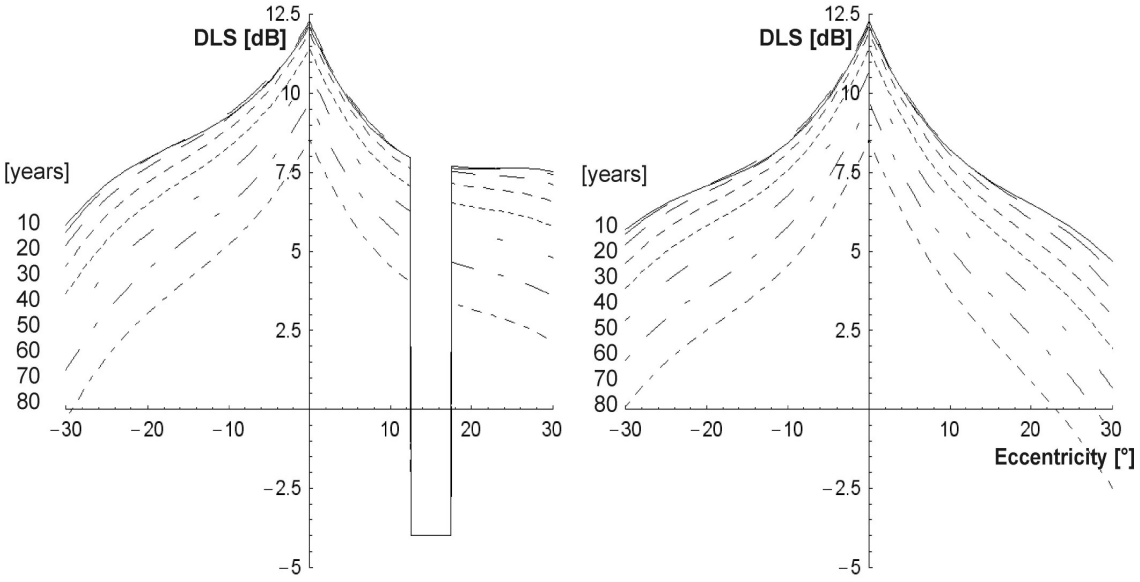

Fig.3: Age effect on the hill of vision in the *horizontal* profile cut (0°-180°, left) and in the *vertical* profile cut (90°-270°, right).

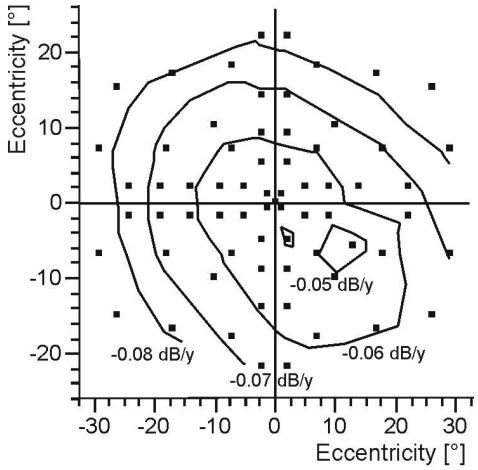

Fig.4: Ageing by visual field location. Aging is more pronounced in the periphery.

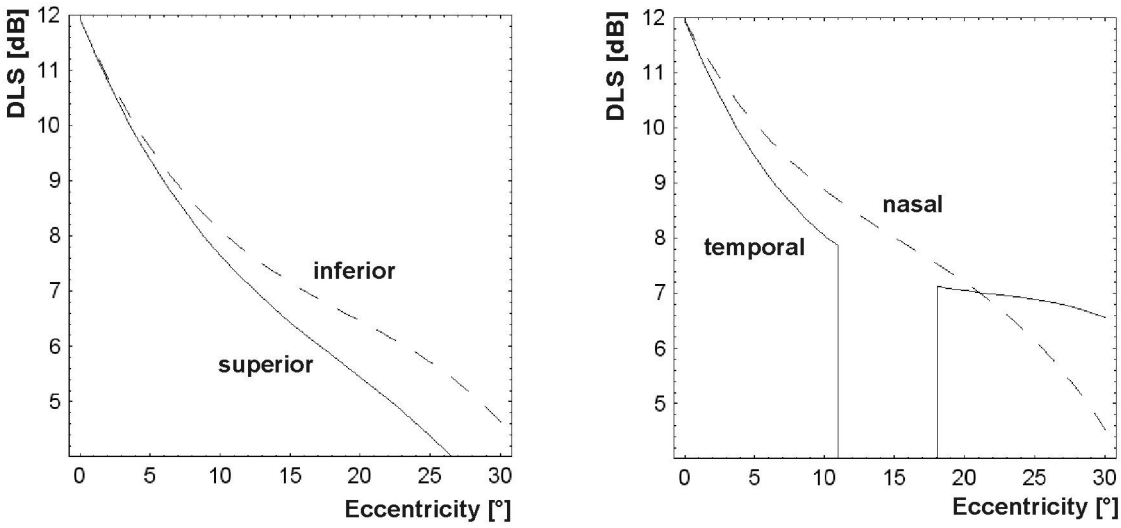

Fig.5: Asymmetries of the hill of vision in the 40 year-olds. Left: *Superior* and *inferior* profile cut (90°-270°), right: *Temporal* and *nasal* profile cut (0°-180°).

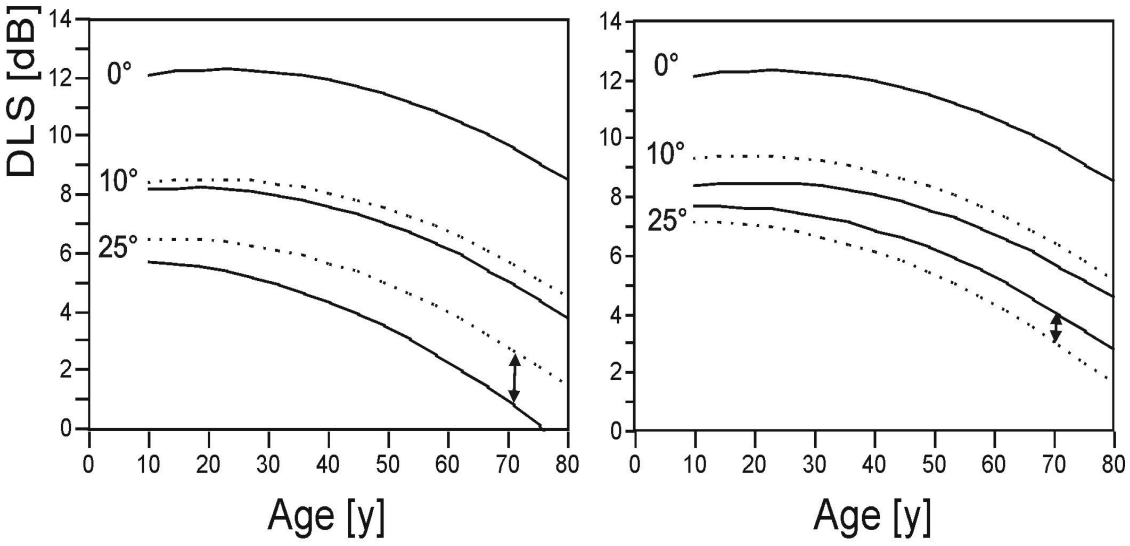

Fig.6: Predicted DLS and indicated eccentricities by age: Left: *vertical* meridian (90°-270°), superior (solid lines) and inferior (dotted lines) hemifield. Right: *horizontal* meridian (0°-180°), temporal (solid lines) and nasal (dotted lines) hemifield. The double-headed arrow indicates the predicted inferior-superior DLS and tempo-nasal asymmetry at an eccentricity of 25° for a 70 year old subject.

Appendix

Model

Four variables: *age*, *eccentricity*, *angle* and *subject* and their interactions define the model. The location in the visual field is given in polar coordinates, i.e, eccentricity and angle of the radial ray.

Model estimation: Differential luminance sensitivity (DLS) = 11.744986
+ 0.0495042 × *age*
– 0.001119 × age^2
– 0.545229 × *ecc*
– 0.005236 × *ecc* × sin(*ang*)
– 0.085799 × *ecc* × cos(*ang*)
+ 0.0045401 × *ecc* × sin(2 *ang*)
+ 0.0233836 × *ecc* × cos(2 *ang*)
+ 0.0234734 × ecc^2
– 0.000393 × ecc^3
– 0.00405 × *age* × *ecc*
– 0.000375 × *ecc* × sin(*ang*) × *age*
+ 0.0001756 × *ecc* × cos(*ang*) × *age*
– 0.000288 × *ecc* × sin(2 *ang*) × *age*
+ 0.0001482 × *ecc* × cos(2 *ang*) × *age*
– 0.000262 × ecc^2× sin(*ang*)
+ 0.0037536 × ecc^2 × cos(*ang*)
– 0.000026 × ecc^2 × *age*
+ *subject*

age = age of the subjects [years]; e*cc* = eccentricity [degrees]; *ang* = angle [degrees]; *subject* = individual coefficient

Meaning of the interactions:

- *age*, age^2: describe the aging process as a parabola
- *ecc*, *ecc* × sin(*ang*), *ecc* × cos(*ang*), *ecc* × sin(2 *ang*), *ecc* × cos(2 *ang*): characterise the dependence of differential luminance sensitivity on *ecc* and *angle*. The interaction of *ecc* and *angle* reproduce the shape of isopters (contours of the same sensitivity), formed by the anatomical and physiological conditions. The apex of the hill of vision is set to the foveola.
    a) *ecc* × sin(*ang*) and *ecc* × cos(*ang*) result in an elliptic isopters, *ecc* × sin(2*ang)* and *ecc* × cos(2*ang*) deform those ellipses.

b) *ecc* × cosine causes a temporal/ nasal deferment of the isopters.
c) *ecc* × sine accounts for a vertical shift of the isopters.
d) e*cc*, ecc^2, ecc^3 constitute a third order polynomial, which is rotated, representing half the profile of the hill of vision with its steep outer slopes and central peak.
e) *age* × *ecc, age* × ecc^2 include the interaction of age and eccentricity, i.e. differential aging.
f) *ecc* × sin(*ang*) × *age, ecc* × cos(*ang*) × a*ge, ecc* × sin(2 *ang*) × *age and ecc* × cos(2 *ang*) × *age* describe a threefold interaction of age and shape of the hill of vision.
g) ecc^2 × sin(*ang*), ecc^2 × cos(*ang*): these terms are considered as higher form parameter, describing curvature and asymmetry of the hill of vision.
h) *subject*: with this individual factor a random effect of subjects is included.

Parsimonious model

Differential luminance sensitivity (DLS) = 13.0593537
– 0.5638668 × *ecc*
+ 0.0223391 × ecc^2
– 0.0003937 × ecc^3
– 0.0781065 × *ecc* × cos(*ang*)
+ 0.0299404 × *ecc* × cos(2 *ang*)
+ 0.0037572 × ecc^2 × cos(*ang*)
– 0.0007396 × age^2
– 0.0005740 × *ecc* × sin(*ang*) × *age*
– 0.00020589 × *ecc* × sin(2 *ang*) × *age*
+ *subject*

age = age of the subjects [years]; e*cc* = eccentricity [degrees]; *ang* = angle [degrees]; *subject* = individual coefficient;

The rotating cubic polynomial is modified in the directions of the main and the oblique meridians only. The elliptical part of the isopters is widest strictly horizontally. (The main axis is not rotated against the horizon.) The quadratic part of the polynomial is modified only horizontally to form the steep slope nasally and the plateau around the blind spot. In this model fit the aging process was simplified to a parabola, which is not tilted, as it is in the previous model. All of the differential aging is described by two three-way interactions without most of the corresponding two-way interactions. Only sine of an angle interacts with

age, showing that the aging process affects the superior and inferior visual field differently.

References

1. Ata N, Sänger A, Dietrich TJ, Selig B, Schiefer U, Benda N (1998) Does age influence inferior-superior or nasal-temporal asymmetry of differential light sensitivity? A campimetric study using bright and dark stimuli. Invest Ophthalmol Vis Sci 39:1092
2. Balazsi AG, Rootman J, Drance SM, Schulzer M, Douglas GR (1984) The effect of age on the nerve fiber population of the human optic nerve. Am J Ophthalmol 97:760-766
3. Benda N, Dietrich TJ, Schiefer U (1997) Gibt es nasal-temporale bzw. superior-inferiore Differenzen der Lichtunterschiedsempfindlichkeit? Ophthalmologe 94 (Suppl. 1):176
4. Brenton RS, Phelps CD (1986) The normal visual field on the Humphrey field analyzer. Ophthalmologica 193:56-74
5. Casson EJ, Johnson CA, Nelson-Quigg JM (1993) Temporal modulation perimetry: the effects of aging and eccentricity on sensitivity in normals. Invest Ophthalmol Vis Sci 34:3096-3102
6. Chauhan BC (2004) Detection of glaucoma:the role of new functional and structural tests. Current Opinion in Ophthalmology 15:93-95
7. Costagliola C, Iuliano G, Rinaldi E, Trapanese A, Russo V, Camera A, Scibelli G (1989) In vivo measurement of human lens aging using the lens opacity meter. Ophthalmologica 199:158-161
8. Curcio CA, Allen KA (1990) Topography of ganglion cells in human retina. J Comp Neur 300:5-25
9. Curcio CA, Millican CL, Allen KA, Kalina RE (1993) Aging of the human photoreceptor mosaic: evidence for selective vulnerability of rods in central retina [see comments]. Invest Ophthalmol Vis Sci 34:3278-3296
10. de Natale R, Flammer J, Zulauf M, Bebie T (1988) Influence of age on the transparency of the lens in normals: a population study with help of the Lens Opacity Meter 701. Ophthalmologica 197:14-18
11. Derefeldt G, Lennerstrand G, Lundh B (1979) Age variations in normal human contrast sensitivity. Acta Ophthalmol Copenh 57:679-690
12. Devaney KO, Johnson HA (1980) Neuron loss in the aging visual cortex of man. J Gerontol 35:836-841
13. Dietrich TJ, Ata N, Sänger A, Selig B, Schiefer U, Benda N (1999) Age influences asymmetry in differential luminance sensitivity. In: Wall M, Wild JM (Hrsg) Perimetry Update 1998/1999. Kugler Publications, Hague, Netherlands pp 223-227
14. Dolman CL, McCormick AQ, Drance SM (1980) Aging of the optic nerve. Arch Ophthalmol 98:2053-2058
15. Dorey CK, Wu G, Ebenstein D, Garsd A, Weiter JJ (1989) Cell loss in the aging retina. Relationship to lipofuscin accumulation and macular degeneration. Invest Ophthalmol Vis Sci 30:1691-1699
16. Drance SM, Berry V, Hughes A (1967) Studies on the effects of age on the central and peripheral isopters of the visual field in normal subjects. Am J Ophthalmol 63:1667-1672

17. Drance SM, Berry V, Hughes A (1967) The effects of age on the central isopter of the normal visual field. Can J Ophthalmol 2:79-82
18. Duane A (1925) Subnormal accommodation. Arch Ophthalmol 54:566-587
19. Egge K (1984) The visual field in normal subjects. Acta Ophthalmol Suppl 169:1-64
20. Flammer J (1985) Normal value in computerized perimetry. In: Whalen WR, Spaeth GL (Hrsg) Computerized visual fields. Slack Inc., Thorofare, NJ pp 159-164
21. Gao H, Hollyfield JG (1992) Aging of the human retina. Differential loss of neurons and retinal pigment epithelial cells. Invest Ophthalmol Vis Sci 33:1-17
22. Gartner S, Henkind P (1981) Aging and degeneration of the human macula. 1. Outer nuclear layer and photoreceptors. Br J Ophthalmol 65:23-28
23. Gloor B, Gloor E (1986) Die Erfaßbarkeit glaukomatöser Gesichtsfeldausfälle mit dem automatischen Perimeter Oktopus. Klin Monatsbl Augenheilkd 188:33-38
24. Goldmann H (1945) Ein selbstregistrierendes Projektionskugelperimeter. Ophthalmologica 109:71-79
25. González de la Rosa M, Reyes JAA, Gonzales Sierra MA (1990) Rapid assessment of the visual field in glaucoma using an analysis based on multiple correlations. Graefes Arch Clin Exp Ophthalmol 228:387-391
26. Greve EL, Wijnans M (1973) The statistical evaluation of measurements in static campimetry and its consequences for multiple stimulus campimetry. Ophthalmic Res 4:355-366
27. Haas A, Flammer J, Schneider U (1986) Influence of age on the visual fields of normal subjects. Am J Ophthalmol 101:199-203
28. Heijl A (1993) Perimetric point density and detection of glaucomatous visual field loss. Acta Ophthalmol (Copenh) 71:445-450
29. Heijl A (2005) The implication of the results of computerized perimetry in normals for the statistical evaluation of glaucomatous visual field. In: Krieglstein GK (Hrsg) Glaucoma Update III. Springer, Berlin pp 115-122
30. Heijl A, Lindgren G, Olsson J (1987) Normal variability of static perimetric threshold values across the central visual field. Arch Ophthalmol 105:1544-1549
31. Heijl A, Lindgren G, Olsson J (1989) The effect of perimetric experience in normal subjects. Arch Ophthalmol 107:81-86
32. Hudson C, Wild JM, O'Neill EC (1994) Fatigue effects during a single session of automated static threshold perimetry. Invest Ophthalmol Vis Sci 35:268-280
33. Interzeag AG (1996) Octopus - Visual field digest. Interzeag AG, Schlieren, Switzerland
34. Iwase A, Kitazawa Y, Ohno Y (1988) On age-related norms of the visual field. Jpn J Ophthalmol 32:429-437
35. Jaffe GJ, Alvarado JA, Juster RP (1986) Age-related changes of the normal visual field. Arch Ophthalmol 104:1021-1025
36. Johnson CA, Adams AJ, Lewis RA (1989) Evidence for a neural basis of age-related visual field loss in normal observers. Invest Ophthalmol Vis Sci 30:2056-2064
37. Katz J, Sommer A (1986) Asymmetry and variation in the normal hill of vision. Arch Ophthalmol 104:65-68

38. Katz J, Sommer A (1987) A longitudinal study of the age-adjusted variability of automated visual fields. Arch Ophthalmol 105:1083-1086
39. Kilbride PE, Hutman LP, Fishman M, Read JS (1986) Foveal cone pigment density difference in the aging human eye. Vision Res 26:321-325
40. Koller G, Haas A, Zulauf M, Koerner F, Mojon D (2001) Influence of refractive correction on the peripheral visual field in static perimetry. In: Wall M, Mills RP (Hrsg) Perimetry Update 2000/2001. Kugler Publications, The Hague/The Netherlands pp 69-70
41. Lachenmayr BJ, Kiermeir U, Kojetinsky S (1995) Points of a normal visual field are not statistically independent. German J Ophthalmol 4:175-181
42. Lachenmayr BJ, Kojetinsky S, Ostermaier N, Angstwurm K, Vivell PMO, Schaumberger M (1994) The different effects of aging on normal sensitivity in flicker and light-sense perimetry. Invest Ophthalmol Vis Sci 35:2741-2748
43. Lachenmayr BJ, Kojetinsky S, Vivell PMO (2001) Is there an accelerated loss at older age for normal sensitivity in the central visual field? In: Wall M, Mills RP (Hrsg) Perimetry Update 2000/2001. Kugler Publications, The Hague/The Netherlands pp 49-56
44. Lewis RA, Johnson CA, Keltner JL, Labermeier PK (1986) Variability of quantitative automated perimetry in normal observers. Ophthalmology 93:878-881
45. Lewis TL, Maurer D (1992) The development of the temporal and nasal visual fields during infancy. Vision Res 32:903-911
46. Lorch L, Dietrich TJ, Schwabe R, Schiefer U (2001) Vergleich der lokalen Lichtunterschiedsempfindlichkeits- (LUE)-Messwerte zwischen dem Oculus-Twinfield-Perimeter und dem Humphrey Field Analyzer (HFA I) Typ 630 - Eine alterskorrelierte perimetrische Normwertstudie. Klin Monatsbl Augenheilkd 218:782-794
47. Marra G, Flammer J (1991) The learning and fatigue effect in automated perimetry. Graefes Arch Clin Exp Ophthalmol 229:501-504
48. Marshall J, Grindle J, Ansell PL, Borwein B (1979) Convolution in human rods: an ageing process. Br J Ophthalmol 63:181-187
49. Métin C, Frost DO (1989) Visual responses of neurons in somatosensory cortex of hamsters with experimentally induced retinal projections to somatosensory thalamus. Proc Natl Acad Sci USA 86:357-361
50. Norren DV, Vos JJ (1974) Spectral transmission of the human ocular media. Vision Res 14:1237-1244
51. Okuyama S, Matsumoto C, Uyama K, Otori T (2001) Reappraisal of normal values of the visual field using the Octopus 1-2-3. In: Wall M, Mills RP (Hrsg) Perimetry Update 2000/2001. Kugler Publications, The Hague/The Netherlands pp 359-363
52. Olsson J, Asman P, Heijl A (1997) A perimetric learner's index. Acta Ophthalmol Scand 75:665-668
53. Parrish RK, Schiffman J, Anderson DR (1984) Static and kinetic visual field testing - reproducibility in normal volunteers. Arch Ophthalmol 102:1497-1502
54. Pokorny J, Smith VC, Lutze M (1987) Aging of the human lens. Applied Optics 26:1437-1440
55. Rabin S, Kolesar P, Podos SM, Wilensky JT (1981) A visual field screening protocol for glaucoma. Am J Ophthalmol 92:630-635

56. Repka MX, Quigley HA (1989) The effect of age on normal human optic nerve fiber number and diameter. Ophthalmology 96:26-32
57. Rosenbach O (1903) Über monoculare Vorherrschaft beim binocularen Sehen. Med Wochenschrift 50:1290-1292
58. Said FS, Weale RA (1959) The variation with age of the spectral transmissivity of the living human crystalline lens. Gerontologia 3:213-231
59. Schiefer U, Flad M, Stumpp F, Malsam A, Paetzold J, Vonthein R, Denk PO, Sample PA (2003) Increased detection rate of glaucomatous visual field damage with locally condensed grids: a comparison between fundus-oriented perimetry and conventional visual field examination. Arch Ophthalmol 121:458-465
60. Schiefer U, Malsam A, Flad M, Stumpp F, Dietrich TJ, Paetzold J, Vonthein R, Knorr M, Denk PO (2001) Evaluation of glaucomatous visual field loss with locally condensed grids using fundus-oriented perimetry (FOP). Eur J Ophthalmol 11:57-62
61. Schiefer U, Malsam A, Flad M, Stumpp F, Dietrich TJ, Vonthein R, Denk PO (2001) Individually condensed grids using Fundus Oriented Perimetry (FOP) increase detection rate of glaucomatous visual field defects (VFDs). Invest Ophthalmol Vis Sci 42:154
62. Schiefer U, Schiller J, Flad M (2003) Konventionelle Perimetrie - Aktueller Stand und künftiges Entwicklungspotential. In: Kampik A, Grehn F (Hrsg) Augenärztliche Diagnostik. Stuttgart, Thieme Verlag pp 93-108
63. Schwabe R, Vonthein R, Ata N, Paetzold J, Dietrich TJ, Schiefer U (2001) Modeling the hill of vision. In: Wall M, Mills RP (Hrsg) Perimetry Update 2000/2001. Kugler Publications, The Hague/The Netherlands pp 71-79
64. Siik S, Airaksinen PJ, Tuulonen A, Alanko HI, Nieminen H (1991) Lens autofluorescence in healthy individuals. Acta Ophthalmol Copenh 69:187-192
65. Sommer A, Quigley HA, Robin AL, Miller NR, Katz J, Arkell S (1984) Evaluation of nerve fiber layer assessment. Arch Ophthalmol 102:1766-1771
66. Stürmer J (1985) What do glaucomatous visual fields really look like in fine-grid computerized profile perimetry? Dev Ophthal 12:1-47
67. Stürmer J, Gloor B, Tobler HJ (1984) Wie sehen Glaukomgesichtsfelder wirklich aus? Klin Monatsbl Augenheilkd 184:390-393
68. Sugimoto K, Schötzau A, Bergamin O, Zulauf M (1997) Optimizing distribution and number of test locations in perimetry. In: Wall M, Heijl A (Hrsg) Perimetry Update 1996/1997. Kugler, Amsterdam/New York pp 101-105
69. Tan KEWP (1971) Vision in the ultraviolet. Thesis, University of Utrecht, The Netherlands
70. van Norren D, van Meel GJ (1985) Density of human cone photopigments as a function of age. Invest Ophthalmol Vis Sci 26:1014-1016
71. Vannas M, Wilska A (1935) Eine Methode zur Messung der Fluoreszenz der lebenden menschlichen Augenlinse und eine Untersuchung über ihre Abhängigkeit vom Alter. Klin Monatsbl Augenheilkd 95:53-64
72. Vivell PMO, Lachenmayr BJ, Schaumberger M, Zimmermann P, Dietrich J, Mueller AJ (1992) Normal data of the central and peripheral visual field for the peristat 433. Invest Ophthalmol Vis Sci 33:969

73. Wabbels BK, Schiefer U (1999) Altersabhängige "Fehlerquoten" bei der automatischen Rasterkampimetrie mit hellen und dunklen Stimuli. Ophthalmologe 96:813-821
74. Wabbels BK, Schiefer U, Treutwein B, Benda N, Stercken-Sorrenti G (1995) Automated perimetry with bright and dark stimuli. German J Ophthalmol 4:217-221
75. Weale RA (1963) The aging eye. Harper and Row, New York
76. Weale RA (1983) Focus on Vision. Harvard University Press, Cambridge, MA
77. Weber J, Kosel J (1986) Glaukomperimetrie – die Optimierung von Prüfpunktrastern mit einem Informationsindex. Klin Monatsbl Augenheilkd 189:110-117
78. Wilensky JT, Joondeph BC (1984) Variation in visual field measurements with an automated perimeter. Am J Ophthalmol 97:328-331
79. Zeimer RC, Noth JM (1984) A new method of measuring in vivo the lens transmittance, and study of lens scatter, fluorescence and transmittance. Ophthalmic Res 16:246-255
80. Zeyen TG, Zulauf M, Caprioli J (1993) Priority of Test Locations for Automated Perimetry in Glaucoma. Ophthalmology 100:518-522
81. Zulauf M, Flammer J, LeBlanc RP (1994) Normal visual fields measured with Octopus programm G1. I. Differential light sensitivity at individual test locations. Graefes Arch Clin Exp Ophthalmol 232:509-515
82. Zulauf M, LeBlanc RP, Flammer J (1994) Normal visual fields measured with Octopus-Program G1. II. Global visual field indices. Graefes Arch Clin Exp Ophthalmol 232:516-522

Danksagung

Für das Gelingen dieser Arbeit schulde ich vielen Menschen meinen herzlichen Dank.
Zunächst möchte ich an alle Probanden erinnern, die sich mit viel Zeit und Einsatz an dieser Studie beteiligten.
Ganz besonders danken möchte ich meinem Doktorvater Prof. Dr. med. U. Schiefer für seine hervorragende Betreuung und seine vielen wertvollen Ratschläge und Ideen.
Großen Dank schulde ich Herrn Dr. rer. nat. J. Paetzold, der stets ein offenes Ohr für meine Fragen hatte und mir immer hilfsbereit zur Seite stand.
Zu danken habe ich auch Herrn Dr. rer. pol. R. Vonthein vom Institut der Medizinischen Biometrie für seine geduldige Hilfe bei den statistischen Auswertungen, seine Experimentierfreudigkeit und seine aufmunternde Art.
Mein Dank gilt auch B. C. Chauhan (PhD), von der Universität Dalhousie (Kanada) für die kritische Durchsicht meines Manuskriptes und seine hilfreichen Verbesserungsvorschläge.
Für die tolle Zusammenarbeit, den regen Gedankenaustausch und das nette Arbeitsklima möchte ich mich bei der gesamten Arbeitsgruppe Sehbahn bedanken. Ganz besonders erwähnen möchte ich Elke Krapp, Bettina Selig und Stephan Rauscher, die mit viel Engagement zum Gelingen dieser Arbeit beigetragen haben.
Der größte Dank gilt allerdings meinen Eltern und meinem lieben Mann Benedikt für ihre unermüdliche Geduld und Unterstützung in dieser Zeit. Ohne sie wäre diese Dissertation nicht möglich gewesen. Ihnen möchte ich diese Arbeit widmen.

Lebenslauf

Agness Matthiesen, geb. Hermann

Geburtsdatum:	4. November 1979
Geburtsort:	Pawlodar, Kasachstan
Eltern:	Dipl.-Ing. Nelli Hermann, geb. Singer und Dr. Ing. Jakob Hermann
Familienstand:	verheiratet mit Benedikt Matthiesen seit dem 22. März 2006
Staatsangehörigkeit:	deutsch

Schulische Ausbildung:

1986 – 1990	Grundschule in Pawlodar
1990 – 1991	Grundschule in Kirchentellinsfurt
1991 – 2000	Wildermuth Gymnasium in Tübingen
2000	Abitur

Universitäre Ausbildung:

2000 – 2001	Studium der Automatisierungstechnik an der Technischen Universität Stuttgart
2001 – 2006	Studium der Humanmedizin an der Eberhardt-Karls - Universität Tübingen
2003	Erster Abschnitt der Ärztlichen Prüfung
2006 - 2007	Praktisches Jahr in Bern (Schweiz) und Reutlingen
06.06.2008	Zweiter Abschnitt der Ärztlichen Prüfung